Cellulose (2023) 30:8739–8751
https://doi.org/10.1007/s10570-023-05362-x

ORIGINAL RESEARCH

Dissolution of viscose rayon multifilament yarn in the ionic liquid 1-ethyl-3-methylimidazolium acetate studied using time–temperature superposition

Maer Alanazi · Michael E. Ries · Peter J. Hine

Received: 8 December 2022 / Accepted: 28 June 2023 / Published online: 11 August 2023

Abstract Wide-angle X-ray diffraction (WAXS) and mechanical testing techniques are used to track the dissolution of a viscose rayon multifilament yarn in the ionic liquid 1-ethyl-3-methyl-imidazolium acetate $[C_2mim]^+$ $[OAc]^-$ for different times and temperatures. In the dissolution process, the oriented cellulose II crystals in the regenerated cellulose fibres dissolve and then reform into randomly oriented crystals to form a matrix phase, and this change in orientation enables us to follow the dissolution process using WAXS, and hence determine the dissolved matrix volume fraction v_m. The change in the average molecular orientation P_2 determined from an azimuthal (α) X-ray scan, allows the growth of the matrix volume fraction v_m to be calculated with time and temperature. The growth of v_m was found to follow time temperature superposition, with an Arrhenius behaviour, giving a value for the activation energy of $E_a = 149 \pm 4$ kJ/mol. Young's modulus was measured on all the resulting processed composites. The fall of Young's modulus with dissolution time and temperature was also found to follow time–temperature superposition, with an Arrhenius behaviour giving a value for $E_a = 198 \pm 29$ kJ/mol. The Young's Modulus results plotted against v_m determined from the WAXS measurements fitted well to the Voigt upper bound parallel Rule of Mixtures .

Keywords Rayon · Ionic liquid · Time–temperature superposition (tts)

Supplementary Information The online version contains supplementary material available at https://doi.org/10.1007/s10570-023-05362-x.

M. Alanazi
Department of Physics, Faculty of Science, University of Tabuk, Tabuk 71491, Saudi Arabia

M. Alanazi · M. E. Ries (✉) · P. J. Hine
School of Physics and Astronomy, University of Leeds, Leeds LS2 9JT, UK
e-mail: M.E.Ries@leeds.ac.uk

Introduction

Cellulose offers the possibility to be a renewable material source with nontoxicity and biodegradability (Kalia et al. 2011). Cellulose fibres can be found as both natural fibres and as man-made fibre: the man-made fibres are known as regenerated cellulose. Regenerated cellulose fibres can be made by dissolving natural cellulose (a mixture of cellulose I crystals and amorphous cellulose), which after dissolution and coagulation results in a mixture of cellulose II crystals and amorphous cellulose (Zugenmaier 2001; Jiang et al. 2020).

Regenerated cellulose fibres, which can be used to produce textile materials, are produced on the industrial scale via the viscose and lyocell processes (Meredith et al. 2013; Shen et al. 2010). Cross and Bevan first discovered the viscous process in 1893 as discussed in papers of (Woodings 2001; Nevell

et al. 1985). The viscous process is based on dissolving wood pulp in sodium hydroxide and using carbon disulphide (CS2) to produce cellulose xanthate (Einsiedel et al. 2010). The cellulose xanthate is subsequently injected into a bath containing sulfuric acid and zinc sulphate (Hermanutz et al. 2019). The lyocell process is based on dissolving wood pulp directly in methylmorpholine-N-oxide (NMMO) monohydrate to get a homogenous solution. The homogenous solution is then spun and stretched in the air gap in the filament form. After that, the fibres are regenerated by coagulating in a mixture of a water/NMMO spin bath, and then washed and dried discussed in papers of (Sayyed et al. 2019; Woodings 2001).

Viscose rayon multifilament yarn is a regenerated cellulose man-made fibre, which can be obtained from wood pulp using the viscous process. Viscose rayon multifilament yarn is considered to be an eco-environmental material. Viscose rayon multifilament yarn was first produced by Glanzstoffwerke in 1938. Viscose rayon multifilament yarn has excellent mechanical properties, which include high temperature resistance and the ability to take high stresses. Therefore, Viscose rayon multifilament yarn have been used in a variety of commercial applications including car tyres, automotive brake hoses and rubber goods (Cordenka 2022).

To dissolve and regenerate cellulose fibres, different solvent systems have been used. The solvent systems such as N, N-dimethylacetamide with Lithium chloride (DMAc/LiCl), and sodium hydroxide with urea (NaOH/urea) have been employed in the dissolution of cellulose (Seydibeyoğlu et al. 2008; Sescousse et al. 2010). However, it has been found that these solvents systems were unable to dissolve high concentrations of cellulose directly (Sescousse et al. 2010; Zhao et al. 2009). For this reason, ionic liquids have found increasing popularity as good solvents to dissolve cellulose. Walden first defined an ionic liquid in 1914 (Pinkert et al. 2009; Walden 1914); an ionic liquid (IL) is a salt which has a melting point below 100 °C (Pinkert et al. 2009; Hall et al. 2012). An organic ionic liquid has attractive properties, in general non-toxic, potential recyclability, thermal stability, and low vapor pressure (Zavrel et al. 2009; Pinkert et al. 2009; Sescousse et al. 2010; Seydibeyoğlu et al. 2008). Ionic liquids can be used in various applications such as electro-elastic materials, heat storage, energy, and chemical analysis (Gupta et al. 2015). In 2002, Swatloski discovered that the ionic liquid 1-butyl-3-methylimidazolium chloride [BIMIM] [Cl]. could directly dissolve cellulose, and can dissolve a high cellulose concentration (Swatloski et al. 2002). It is worth noting that the purity of the IL (95% in our case) could also affect the dissolution due to additional side reactions or derivatizing reactions; (Liebner et al. 2010) caution that additional side reactions with cellulose can occur if the IL contains significant impurities. Furthermore, (Zweckmair et al. 2015) describe how acetylation reactions can occur with cellulose for aged ILs (they studied 1,3-dialkylimidazolium acetate) with resultant impurities. They propose that pure ILs do not show this reaction.

Ionic liquid systems based on the imidazolium ring have excellent properties, such as low viscosity and high thermal stability (Ghandi 2014). A common ionic liquid based on the imidazolium ring such as 1-ethyl-3-methylimidazolium acetate [C2mim] + [OAc]- has been extensively utilized to dissolve cellulose (Zavrel et al. 2009; Liu et al. 2012). This is due to excellent properties of the IL [C2mim] + [OAc]- such as low melting point and being biodegradable (Sun et al. 2009). This ionic liquid has the ability to dissolve a high concentration (~ 20 wt.%) of cellulose (Köhler et al. 2007).

The structure of regenerated cellulose fibres is often comprised of oriented cellulose II crystals and a randomly oriented amorphous phase (Shen et al. 2010). As the regenerated cellulose fibres dissolves, the oriented cellulose II crystals are transformed into randomly oriented cellulose crystals after coagulation. By analysing the decrease of the cellulose II crystalline orientation (specified by the Herman's Orientation Factor P_2) then the rate of dissolution can be followed with time and temperature. This paper aims to understand the dissolution mechanism of a Viscose rayon multifilament yarn in the Ionic liquid-1-ethyl-3-methyl-imidazolium acetate [C2mim] + [OAc]. This was achieved and compared using two methods, by following the change in both the average crystal orientation using an azimuthal (α) X-ray scan to measuring the 2nd Legendre polynomial function (P_2), and the change in the Young's modulus of dissolved and regenerated 'composites' with time and temperature. The reduction in both parameters were found to follow time–temperature superposition (Cotts et al. 1969), allowing the activation energy of dissolution to be calculated independently by these

two methods. In addition, the two measurements were combined to show that the modulus of the partially dissolved regenerated 'composite' multifilament yarn followed closely to the rule of mixtures. The ultimate aim of the research will be to manufacture all cellulose composites from regenerated cellulose fibres, although this is not reported in this current paper, where the focus is to understanding the physics of the dissolution process and how to use this in the future, to control and tailor properties of composites.

Experimental materials and methods

Materials and sample preparation of composite filaments

The Viscose rayon multifilament yarn (commercial name Cordenka) of regenerated cellulose were provided by Bristol University. The ionic liquid 1-ethyl-3-methyl- imidazolium acetate $[C_2mim]^+$ $[OAc]^-$ with purity 95% was purchased from Sigma Aldrich. The Cordenka filaments sample were dissolved in the IL $[C_2mim]^+$ $[OAc]^-$ at various temperatures and for different times as follows: at 30°C, for 1, 2, 3 and 5 h, at 35°C for 30 min, 1, 2, 3 and 5 h, and at 40°C for 1, 2 and 3 h. Finally, 45°C for 30 min, 1 and 1.5 h.

The unprocessed viscose rayon multifilament yarn (which were untwisted) were wound around a frame, as shown in Fig. 1. Three samples were made for measuring x-ray diffraction and three samples for mechanical measurements. A PTFE dish containing the IL $[C2mim]^+[OAc]^-$ was preheated in a vacuum oven at 1 h for each processing temperature (30, 35, 40, and 45 °C). After this preheating step the samples were put into the dish of IL $[C_2mim]^+$ $[OAc]^-$ and then left in the vacuum oven at the same temperature for set times. The last step was to wash (and coagulate) the processed partially dissolved composites, while still on the frames to remove all the ionic liquid by soaking in water for 24 h, followed by a final drying process on a hot plate at 120 °C for 1 h.

Preparation of film sample

For preparing a fully dissolved sample (which is proposed as representative of the matrix phase of the partially dissolved multifilament), the viscose rayon multifilament yarn was cut into small pieces and then submerged into [C2mim] + [OAc]- with a magnetic stirrer at a speed of 90 rpm, for 48 h at 90 °C on a hot plate, as shown in Fig. 2a. The solution had a total concentration of 19:1 IL [C2mim] + [OAc]- to regenerated cellulose multifilament. The IL was then spread evenly into a 5 cm × 5 cm polystyrene petri dish and left for 30 min in a vacuum oven at 90 °C, to remove any bubbles from the film. This petri dish with solution was put on an upside-down beaker, and then put it in a larger beaker filled with water and sealed, heated at 90 ℃ using a hot plate, for 24 h as shown in Fig. 2b. The water was evaporated slowly inside the beaker to slowly coagulate the film. The resultant film was then washed with water for 24 h,

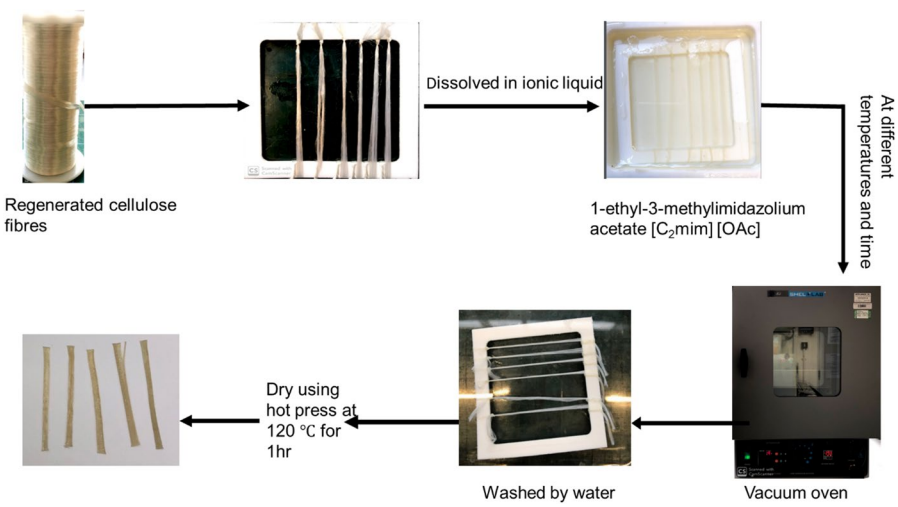

Fig. 1 Dissolution procedure for viscose rayon multifilament yarn

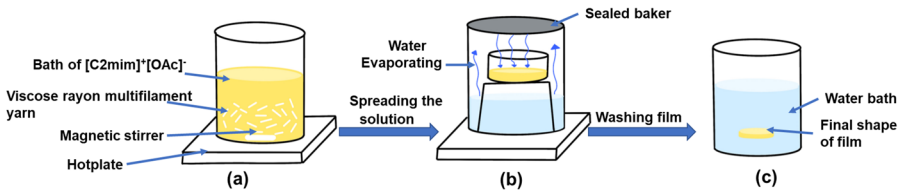

Fig. 2 The preparation of viscose rayon film

to remove any residual ionic liquid. We are making the assumption that after washing the residual IL is at a significantly low enough fraction to not affect mechanical properties, giving a resultant film with light yellow colour as shown in Fig. 2c, and finally this film was dried at 120 ℃ for one hour, using a hot press machine under a minimal contact pressure. This film is considered to be similar to the matrix phase within the viscose rayon composite multifilament yarn.

Experimental methods

Wide angle x-ray diffraction

The degree of orientation within the unprocessed multifilament yarn, the film and the processed composite samples was determined using Wide-Angle X-ray Diffraction (WAXD) with Cu Kα radiation (λ = 1.54 Å) at 40 kV and 30 mA (DRONEK 4-AXES, Huber Diffractions Technik GmbH & Co. KG, Germany). Qualitative measurements of the change in crystalline structure and orientation were obtained by capturing a 2D image of each sample. This was done by passing x-rays through the sample and capturing the resulting pattern on an x-ray sensitive film placed 5 cm away. The exposure time was 3 h.

Quantitative measurements of crystal structure and orientation were carried out using a Huber goniometer and x-ray detector. The 2 θ equatorial scans from 5° to 40° were carried out with a counting time of 40 s per step (0.1°) with the processed composites located in the vertical direction. This allowed the crystalline structure to be confirmed and then enabled the choice of the most appropriate Bragg peak for the circumferential scans. The orientation degree of the crystals was then determined by setting the 2θ angle at 20.3°, which is the position with the maximum count rate and so has the best signal/noise ratio. Circumferential scans were carried out at increments of 5° with an interval time of 30 s per step, with azimuthal angles from −90° to + 90°. For the circumferential α scan, a number of processed composite filaments were placed side by side in the WAXS sample holder to increase the signal to noise ratio.

The crystal structure of the viscose rayon multifilament yarn is transformed from an aligned crystalline structure to randomly oriented crystals in the coagulated phase. Experimentally, the azimuthal α scan is used to measure the orientation of the crystal structure of the processed composites. Once the intensity distribution is measured, then we can determine an average orientation of the crystal's fibre $< cos^2\alpha >$ by using:

$$\left\langle \cos^2 \alpha \right\rangle = \sum_{-90}^{+90} \left(\frac{I(\alpha) \cos^2 \alpha \mathrm{d}\alpha}{I(\alpha)\mathrm{d}\alpha} \right) \tag{1}$$

where $I(\alpha)$ indicates the intensity distribution and α is the angle formed by the fibre axis and reference direction. The average orientation of the processed composites can then be further quantified using the second-order coefficient of Legendre polynomial P_2 (cos α).

$$f = \langle P_2(\cos \alpha) \rangle = \left(3 \left\langle \cos^2 \alpha \right\rangle - 1 \right) / 2 \tag{2}$$

Equation 2 is known as Herman's orientation factor function (f) of the crystalline material (Ellison et al. 2008; Zhu et al. 2016). When $f = 1$ this indicates that crystallites have a perfect alignment, and when $f = 0.25$ the crystallites are completely randomly oriented in a 2D plane, and in the case of $f = -0.5$ molecules crystallites are oriented perpendicular to the axis of the sample (Rusznák et al. 1975).

Young's modulus measurements

The Young's modulus of the processed composite samples was measured using an electromechanical tensile machine Instron 5564 with the Bluehill™

version software employed. The load cell was 2000 N and a crosshead speed of 10 mm/min was used. The cross-section area (m^2) of each processed composites was determined using a gravimetric technique measured by equation:

$$A = \frac{m}{l\rho} \tag{3}$$

where l is the length of fibre and ρ is the density of cellulose, which has been recorded as 1400 kg/m^3 (Mwaikambo et al. 2001; Sun 2005), and m is the mass of fibre. End tabs to give good load transfer were formed using paper and superglue. The sample to be tested was then fixed between two clamps with sandpaper, after measuring the gauge length. Young modulus measurements were repeated three times for each set of processing temperature and processing time to reduce human error and sample to sample variability.

Experimentally, an Instron tensile test machine was used to determine the force–displacement of each sample, and then calculate the Young's Modulus from the relationship between measured stress and strain of the sample displacements δ (Gu et al. 2014).

Results and discussion

Wide angle x-ray diffraction

Two-dimension x-ray diffraction pattern

Cellulose II has three Bragg peaks located at 20.16° and 21.76° and with small peak at 12° (Ohira et al. 2012). A two-dimensional diffraction pattern was captured to determine qualitatively the crystalline structure of the unprocessed multifilament yarn using x-ray sensitive photographic films. Quantitative measurement of the crystal orientation was obtained from an α circumferential scan setting in two dimensions (2D) from −90° to 90° at 2θ = 20.3°. The results of 2D x-ray image showing the positions and reflection peaks are showed in Fig. 3, where the dark arcs correspond to Bragg beaks. There were peaks with reflections $1-10$, 110, 020 which are positioned at 12.4°, 20.2°, 21.8° of 2θ angles respectively for cellulose II. There is another reflection peak which appears in cellulose, which is due to the 012 planes, and can be seen in the 2D x-ray scattering at a circumferential

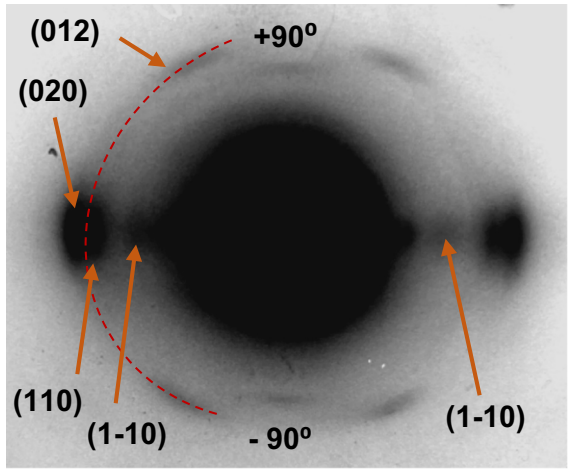

Fig. 3 2D X-ray scattering pattern from unprocessed multifilament yarn showing the α circumferential scan setting in two dimensions (2D) from -90° to 90° (red dashed line) at 2θ = 20.3° and how this includes the 012 reflection

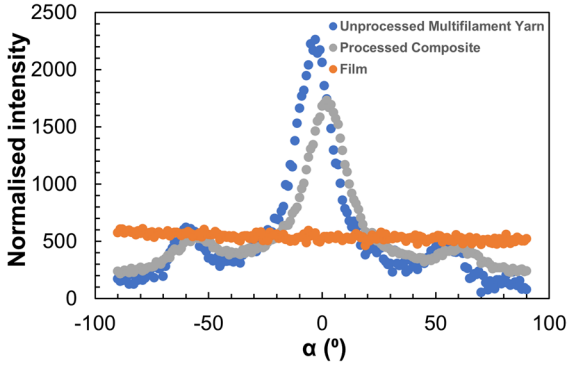

Fig. 4 The azimuthal α scan to measure the change in orientation

angle of ~ ±60° (see also Fig. 4) and a 2θ value of 20.3° as described in ref (Nam et al. 2016). As this 012-reflection plane has a very similar value of 2θ to the chosen equatorial position with maximum signal intensity (20.3°), then this reflection will appear in a circumferential α scan (as shown schematically in Fig. 4). We have proposed to include both these reflections in the determination of P_2 from a numerical integration between -90 and + 90. Our hypothesis is that following the change of any appropriate parameter with time and temperature, allows us to investigate time–temperature superposition and determine an activation energy for dissolution.

2θ scan and azimuthal α scan of viscose rayon multifilament yarn

The measurements of 2θ scan of Viscose rayon multifilament yarn examined the changes of crystal structure during the dissolution and subsequent coagulation process. Experimentally, it was found that the 2θ line scan for the three materials (unprocessed multifilament, processed composites and a film) were not significantly different, as shown in Fig. SI1, and so could not be used to follow change in crystal structure during the dissolution/coagulation process as we have done before in our previously published work on the dissolution of cotton filaments (Liang et al. 2021), which is predominantly cellulose I. Therefore, an alternative method is proposed to calculate the volume fraction of dissolving Viscose rayon multifilament yarn, which was to use the azimuthal α scan to follow the change of crystal orientation with time and temperature. This technique has worked successfully for silk fibres, as has been demonstrated in a previous publication from our research group (Zhang et al. 2021).

The x-ray technique for the azimuthal α scan was carried out from -90° to 90° at a fixed angle 2θ of 20.3° as mentioned above. The measurement of the azimuthal α scan allowed a measurement of the degree of molecular orientation in the various samples. As described above in Fig. 3, and as seen in Fig. 4, such a circumferential scan picks up both the equatorial peak reflection (α = 0°) (which is actually a combination of the 110 and 020 Bragg peaks) and then outer peaks from the 012 reflections as shown in this ref (Nam et al. 2016). It can be seen that the dissolution of the processed composites influenced the intensity of the crystalline reflections. As the oriented crystals (associated with the unprocessed multifilament yarn) dissolved and then they reformed as random crystals, leading to an increase of the background level. For the film sample, a constant intensity was seen at all angles, indicating random orientation of the crystal structure.

The overall average of P_2 for all processed composites, from processing at different times and temperatures, was calculated by using Eq. 2. The results of the change in the average value of P_2 with temperature and time are shown Fig. 5. The reduction in the average P_2 value for processed composites is due to the increasing in the random molecular orientation component due to the dissolved and coagulated matrix fraction. From Fig. 5, It can be seen that the P_2 of the processed composites has reduced with increased time and temperature. The reduction of the average value of P_2 of the processed composites at various times and temperatures appears broadly linear, although with an increasing slope as the processing temperature increases. This indicates increased effectiveness of $[C_2mim]^+$ $[OAc]^-$ to dissolve the viscose rayon multifilament yarn with increasing time and temperature.

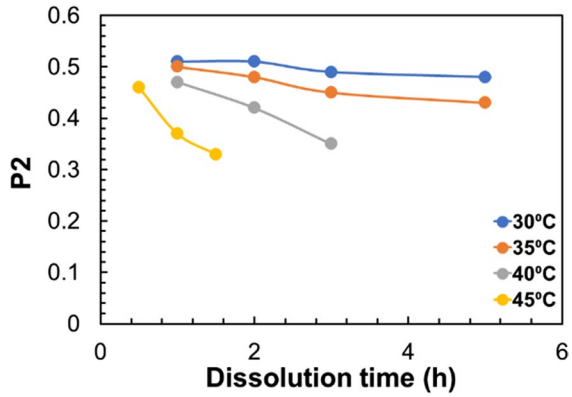

Fig. 5 The calculated P_2 and different dissolution times and temperatures for processed composites

The P_2 data can be formed into a master curve using the concept of time–temperature superposition. This method was previously reported in the study of the dissolution of cotton and silk fibres in $[C_2mim]^+$ $[OAc]^-$ by our research group (Liang et al. 2021; Zhang et al. 2021). Based on this previous work the data of P_2 values are first plotted as function of the logarithm of time and the different temperature curves are then superposed in (ln time) using Eq. 4 at a chosen reference temperature.

$$t_R = t_1 a_T$$

$$\ln t_R = \ln t_1 + \ln a_T \tag{4}$$

where T_1 is the temperature, T_R is reference temperature, t_1 is the time value before scaling, t_R is the time value after scaling/shifting, and ln a_T is the shift factor (Zhang et al. 2021). Figure 6a explains the steps used to find the best shift factors so that all the points overlap on one master curve. Firstly, the orange line at a processing temperature of 35 °C was chosen as the reference temperature (T_R) on the ln time axis

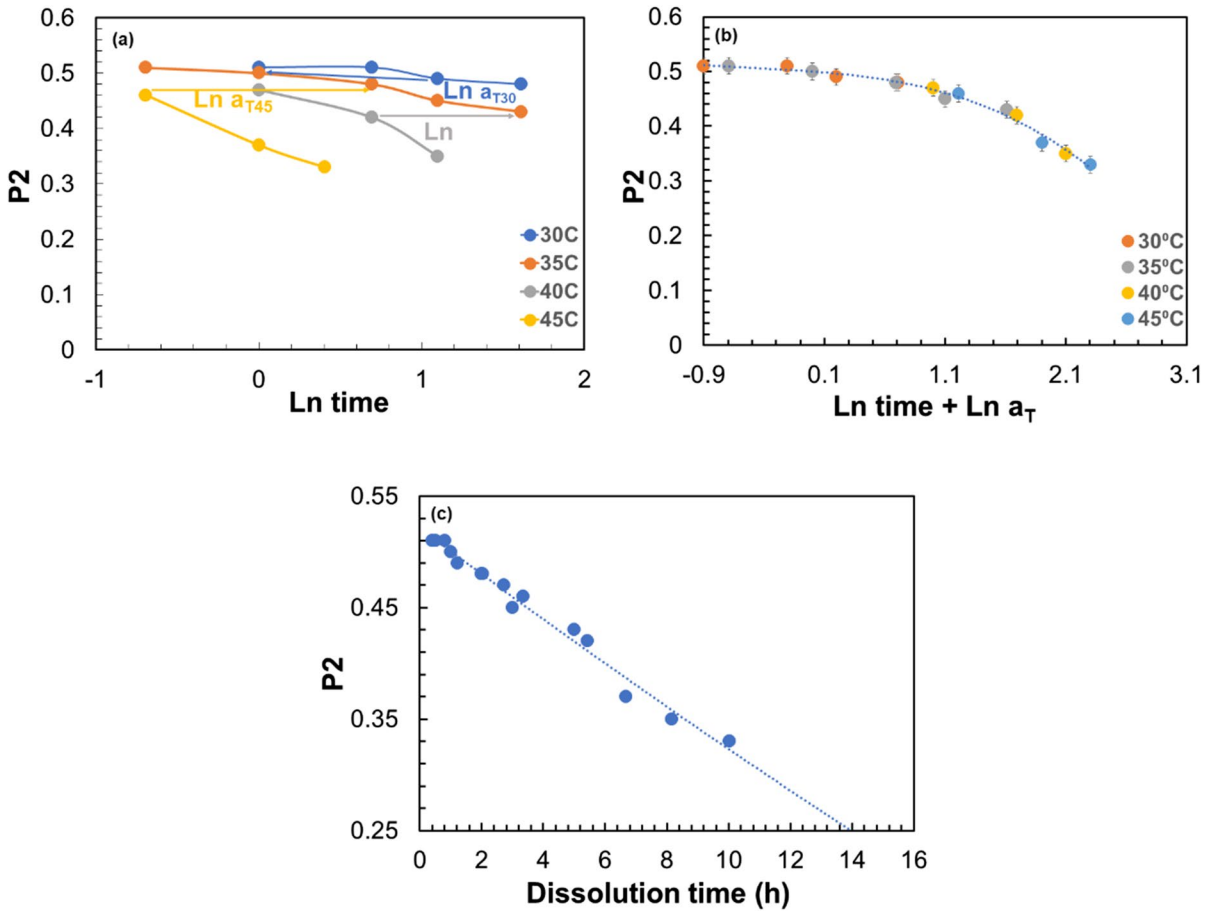

Fig. 6 **a** Logarithm of time (ln a_T) with P_2, all data of time and temperature shifted at reference 35 °C. **b** the master curve of relation between P_2 and shifting time at various temperatures of viscose rayon multifilament yarn. **c** the resultant master curve between P_2 and dissolution time

(Fig. 6a). Then all the other temperature curves were shifted horizontally by an initial shift factor (ln a_T) to the data at 35 °C curve along the ln time, x-axis. Next, a polynomial function was introduced as a guide around this preliminary shifted data. Then the individual shift factors were changed to get the best fit between the polynomial function and the shifted points by maximizing the value of R^2. The final master curve between the average P_2 and the shifted data at a reference temperature of 35 °C, is shown in Fig. 6b.

From the relation between the shifted average P_2 values (at a reference temperature of 35 °C) with linear dissolution time, as shown in Fig. 6c, it can be estimated that complete dissolution of the Viscose rayon multifilament yarn would be achieved after 14 h dissolution time at 35 °C, as the P_2 value of completely dissolved Viscose rayon multifilament yarn extrapolates to 0.25.

Figure 7 shows that plotting the ln of the shift factors versus the inverse temperature gives a linear relationship, indicating that the dissolution of the Viscose rayon multifilament yarn follows an Arrhenius behaviour. We can therefore use Eq. 5 to calculate an activation energy for this dissolution through the Arrhenius equation, as follows:

$$\ln a_T = \ln A - \frac{E_a}{RT} \tag{5}$$

where a_T is the simple multiplicative factor, E_a is the activation energy, R is the universal gas constant and

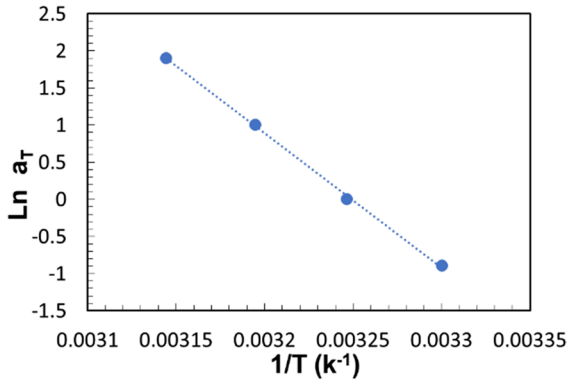

Fig. 7 lna_T plotted against the inverse of temperature, dotted line is Arrhenius equation

T is temperature (K) (Ries et al. 2014; Laidler 1984). Figure 7 shows the best fit line to this data (using the LINEST function in Excel) resulting in an activation energy value of 151 ± 3 kJ/mol. This value quantifies the temperature dependence of dissolution, which is a useful parameter in controlling the fraction of matrix formed when creating an all-cellulose composite to obtain the optimum balance of mechanical properties.

Dissolved and coagulated matrix fraction v_m from wide angle x-ray diffraction

By applying a rule of mixtures to the experimental data of P_2, from the azimuthal α scan measurements, the volume fraction v_m of the dissolving fraction of the original composite multifilament could then be calculated. This dissolved and coagulated fraction (v_m) now indicates the amount of 'matrix' phase resulting in the processed composites combined with the unprocessed multifilament yarn. This procedure was done by calculating the points between the orientation of the unprocessed multifilament yarn with (v_m) = 0% dissolved and the completely dissolved matrix with (v_m) = 100%, by assuming a linear mixing rule as given by:

$$v_m = \frac{p_{2c} - p_{2f}}{p_{2m} - p_{2f}} \tag{6}$$

assuming $v_m + v_f = 1$. Here p_{2c} indicates the P_2 value of the processed composites, p_{2f} is the P_2 value of the unprocessed multifilament (measured as = 0.57) and p_{2m} is the P_2 value of the completely dissolved matrix (film) with 0.25 (randomly oriented crystals).

Figure 8a presented the relationship between the calculated v_m value and the dissolution time and temperature. The volume fraction of dissolved viscose rayon multifilament yarn increases with increasing time and temperature. As carried out above, the data of v_m is likewise shifted with time and temperature, using the temperature of 35 °C as the reference temperature. Once again, this data was found to collapse to a single master curve, as would be expected as it is mathematically based on the P_2 data. The volume fraction as function of time temperature after superposition is shown in Fig. 8b. From the relation between the volume fraction of v_m with linear dissolution time, as shown in Fig. 8c, it can be seen that the complete dissolution of the Viscose rayon multifilament yarn would be achieved after 14 h dissolution time at 35 °C, as the V_m value of completely dissolved Viscose rayon multifilament yarn extrapolates to 1, as shown in Fig. 6c. Figure 8d shows that plotting lna_T against the inverse of temperature gives a linear relationship and from this the activation energy value was calculated by applying the Arrhenius (Eq. 5). The value obtained was 149 ± 4 kJ/mol, which is very close to that found from the time temperature superposition of the average P_2 values, as expected, nevertheless it is a confirmation of our time temperature superposition approach since the two data sets were analysed independently.

Mechanical measurements

The measured Young's modulus of the processed composites as a function of time at various temperatures is shown in Fig. 9a and typical stress–strain curves are shown in Fig. SI2. It can be seen that the pattern of the decrease of the measured Young's modulus values, with time and temperature, is very similar to that shown on Fig. 5 for the measured average P_2 values, as both are a measure of the remaining fraction of the unprocessed filaments. The data of the measured Young's modulus is next shifted with time and temperature, using the temperature of 35 °C as the reference temperature using the same procedure as explained above. Figure 9b, shows the result of the final master curve after shifting the data, plotted against Ln (time).

The relationship between the shifting factors and the inverse temperature was again used to calculate an activation energy (as they showed a linear

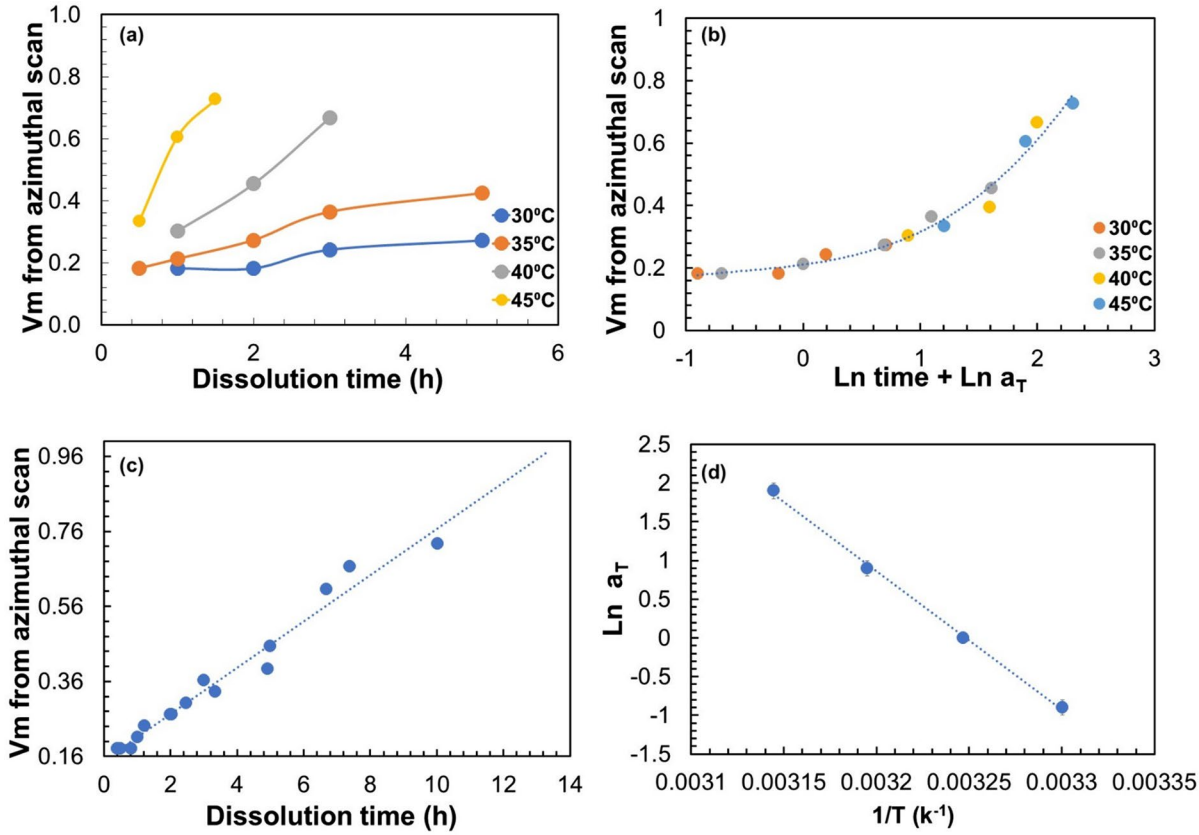

Fig. 8 **a** The relationship between V_m and dissolution time, **b** the master curve of relation between V_m and shifting time at various temperatures of Viscose rayon multifilament yarn. **c** the resultant master curve between V_m and dissolution time. **d** the $\ln a_T$ plotted against the inverse of temperature and resulting an activation energy

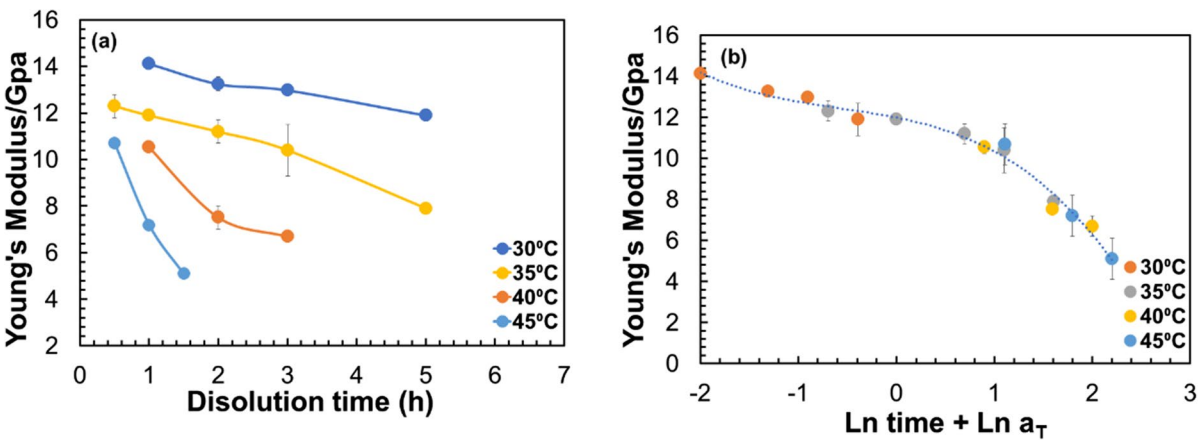

Fig. 9 **a** The measurements of Young's modulus at various temperature and time. **b** the master curve between Young's modulus and dissolution time

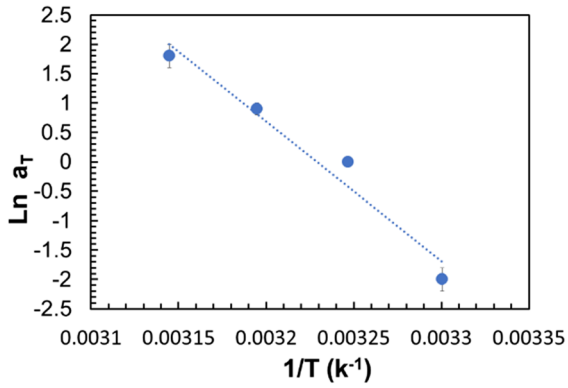

Fig. 10 Activation energy determined from TTS

Table 1 The comparison between the values of E_{P_2} and E_{V_m} and the E_E

35°C	P_2	V_m	E
$E_a kJ/mol$	151 ± 3	149 ± 4	198 ± 29

dependence) using the Arrhenius Eq. 5, see Fig. 10. This gave an activation energy value of 198 ± 29 kJ/mol.

By comparing these three methods, the values of the activation energies of P_2 and the activation energies of volume fraction V_m are similar and lower than the activation energy from analysing the measured Young's modulus data, as shown in Table 1. It is seen that there is a much larger uncertainty in the calculated activation energy based on the Young's modulus measurements.

The relation between the Young's modulus with linear dissolution time in the ionic liquid [C2mim] + [OAc]-, is presented in Fig. 11 for a reference temperature of 35 °C. At short times, the Young's modulus is seen to first fall rapidly, and then, the Young's modulus decreases at a slower, but linear, rate with time. We propose that this is because at early dissolution times, when the individual viscose rayon multifilament yarn are not connected (being untwisted as described earlier), the ionic liquid can penetrate more easily between each individual multifilament, enabling the surrounding outer layer of each multifilament to be dissolved to form the matrix. Once the inner space between the individual multifilament yarn is filled with a dissolved cellulose/[C2mim] + [OAc]-gel, we

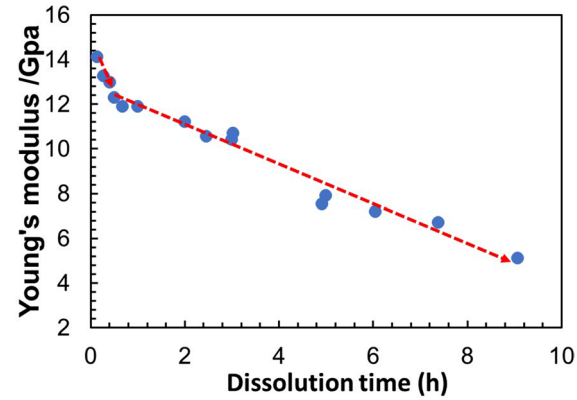

Fig. 11 Master curve between Young's modulus and dissolution time using 35 °C

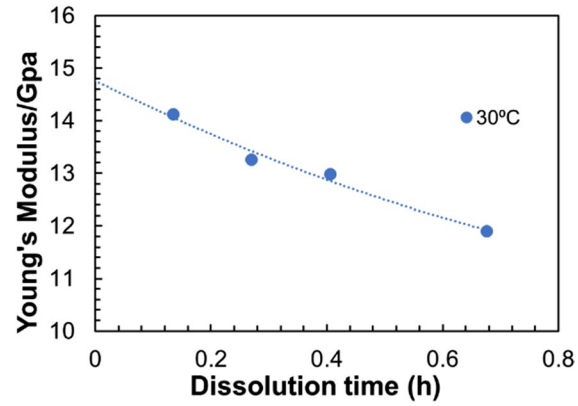

Fig. 12 The extrapolation method to determine the modulus for unprocessed multifilament yarn from Young's modulus master curve at 30 °C

propose that this forms a barrier to the ionic liquid and therefore dissolution proceeds more slowly by now only dissolving the multifilament yarn on the outside of the fibre bundles and so proceeding at a slower rate.

To obtain a value of the modulus of the unprocessed multifilament yarn the data for the early times (the first four points shown in more detail in Fig. 12) are used to extrapolate the modulus to zero time. From the correlation between the Young's modulus data and the linear dissolution time at 30 °C, and using a second order polynomial function, the best fit gave a value of 14.8 GPa for the unprocessed multifilament bundle (limit t tends to zero).

Experimentally, the azimuthal α scan technique has been used to calculate the volume fraction of processed composites of the partially dissolved multifilament. The measured Young's modulus data could then be plotted against these calculated volume fraction values from the azimuthal α scan measurements to evaluate the possibility of applying rule of mixtures to our processed composites, and to specify the effect of changing the volume fraction on the behaviour of the Young's modulus results. The upper-bound (Voigt series), which is also called the parallel rule of mixture and the lower-bound (Reuss series) are used to estimate the effective stiffness of the two phases, fibre and matrix. The Voigt series assumes that the two composite phases have the same strain, while Reuss series assume two phases of composite have the same stress (Lakes et al. 2002; Luo 2021).

The result of plotting the measured Young's modulus and the calculated volume fraction (from the α scan) with the two mixing rules is shown in Fig. 13. Based on the extrapolated fibre value of E_f =14.8 GPa with using $v_m = 0\%$ dissolved and the completely dissolved matrix $v_m = 100\%$, with value of E_m =1.5 GPa (from measuring the film), the upper-bound and lower-bound are calculated by the following equations respectively:

$$E_C = E_m V_m + E_f V_f \tag{7}$$

$$E_C = \frac{1}{(1 - V_m)/E_f + \left(V_m/E_m\right)} \tag{8}$$

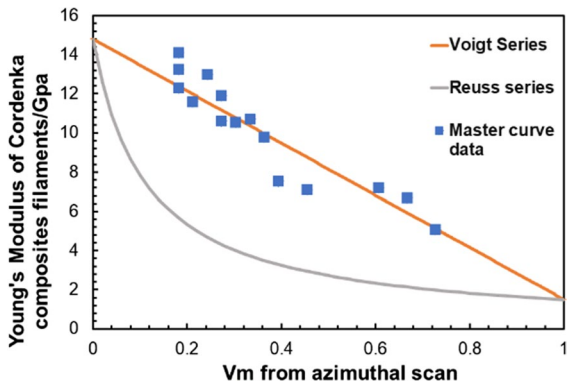

Fig. 13 Relation between volume fraction v_m and Young's modulus from α scan with prediction of rule of mixtures, Voigt and Reuss series

where E_C indicates the young modulus of processed composites in the fibre direction, E_f is the young modulus of 100% multifilament yarn and E_m of a completely dissolved 'matrix' multifilament yarn, assuming $v_m + v_f = 1$. The data points of Young's modulus versus v_m have excellent agreement with the upper- bound (Voigt series), confirming excellent adhesion between the unprocessed multifilament yarn and the dissolved and coagulated matrix fraction. This is an important finding for future work on all cellulose composites made from regenerated cellulose fibres as it demonstrates good bonding can be achieved.

Conclusion

Wide-angle X-ray diffraction and mechanical test techniques have been used in this research to follow quantitatively the physics of the dissolution, and the resulting mechanical properties of multifilament yarn of Viscose rayon. This was done by dissolving the viscose rayon multifilament yarn in an ionic liquid of 1-ethyl-3- methylimidazolium acetate [C2mim]+[OAc]- for different times and temperatures. An azimuthal α scan was employed to determine the dissolution mechanism of the viscose rayon multifilament yarn. The azimuthal α scan at an angle 2θ=20.3° (position of maximum equatorial intensity) was used to follow the change in the crystal orientation with time and temperature of dissolution and hence calculate the volume fraction of the dissolved fraction. The P_2 value of the unprocessed multifilament yarn was found to be 0.57 while the P_2 value of film was measured to be 0.25, which is the expected value for a perfectly random crystalline orientation in a 2D plane. The measured value of P_2 for the partially dissolved composites was found to decrease as time and temperature increased, indicating an increase in the random orientated crystal fraction associated with the dissolved and coagulated matrix fraction. The rule of mixtures was applied to the measured P_2 values to calculate the volume fraction v_m of viscose rayon multifilament yarn dissolving, using the data from the azimuthal α scan for processed composite samples.

The Young's modulus values of the processed composites were also measured for different processing times and temperatures. The time–temperature superposition method was applied to the

experimental data of the average P_2 values, the calculated matrix volume fraction v_m and the processed composites Young's modulus values. Each data set transformed used time–temperature superposition to form a master curve and then the activation energy was calculated by using an Arrhenius equation (all three measured followed Arrhenius behaviour). The activation energies for the three measures, P_2, volume fraction v_m and Young's modulus were found to be 151 ± 3 kJ/mol, 149 ± 4 kJ/mol, and 198 ± 29 kJ/mol, respectively. The activation energies measured from different methods gave similar values, which indicates they could all be used to follow the dissolution behaviour of the Viscose rayon multifilament yarn. By extrapolating the Young's modulus of the processed composites at low temperatures and early times, the modulus of the unprocessed multifilament yarn was measured to be $E_f = 14.8$ GPa, which can often in practice be a difficult parameter to measure. Combining this with the modulus of a completely dissolved and coagulated film, allowed the Young's moduli of the processed composites to be tested against the rules of mixture. The correlation between volume fraction (from the P_2, measurements) and the Young's modulus agreed very well with the predicted parallel rule of mixtures.

Acknowledgments I gratefully acknowledge the Cultural Attaché of Saudi Arabia to the UK and University of Tabuk, Tabuk, Saudi Arabia, for providing me with fellowship for my studies. I would thankful Daniel Baker, Experimental Officer in the school of Physics and Astronomy as well as my colleagues Xin Zhang, James Hawkins and Yunhao Liang for being helpful and supportive.

Authors' contributions MA: Methodology, formal analysis, investigation and writing–original draft. MER: Supervision, conceptualization, writing–review & editing, project administration. PJH: Supervision, conceptualization, writing–review & editing, project administration.

Funding This research was funded by studentship from University of Tabuk, Tabuk, Saudi Arabia.

Data Availability The datasets generated during and/or analysed in the current study are available from the corresponding author on request. The data for all the Figures presented can be found here: https://doi.org/10.5518/1276.

Declarations

Competing interests The authors declare no competing interests.

Consent for publication All the authors have given consent for this publication, which includes text, photographs, figures and details within the text to be published in the journal "Cellulose".

References

Cordenka. 2022. *Reinforcement of tires and other rubber products* [Online]. Available: https://www.cordenka.com/en/rayon-cord-and-fabric [Accessed].

Cotts R, Hoch M, Sun T (1969) Markert J (1989) Pulsed field gradient stimulated echo methods for improved NMR diffusion measurements in heterogeneous systems. J Magn Reson 83:252–266

Einsiedel R, Uihlein K, Ganster J, Rihm R. Cordenka Reinforced PLA—Advanced Bio-derived Composite Material. Konferenzmaterialien: Annual Technical Conference, 2010.

Ellison MS, Lopes PE, Pennington WT (2008) In-situ X-ray characterization of fiber structure during melt spinning. J Eng Fibers Fabr 3:155892500800300300

Ghandi K (2014) A review of ionic liquids, their limits and applications. Green Sustain Chem 4:44–53

Gu B, Burgess DJ (2014) Polymeric materials in drug delivery. Elsevier, Natural and Synthetic Biomedical Polymers

Gupta KM, Jiang J (2015) Cellulose dissolution and regeneration in ionic liquids: a computational perspective. Chem Eng Sci 121:180–189

Hall CA, Le KA, Rudaz C, Radhi A, Lovell CS, Damion RA, Budtova T, Ries ME (2012) Macroscopic and microscopic study of 1-ethyl-3-methyl-imidazolium acetate–water mixtures. J Phys Chem 116:12810–12818

Hermanutz F, Vocht MP, Panzier N, Engineering BMR (2019) Processing of cellulose using ionic liquids. Macromol Mater Eng 304:1800450

Jiang X, Bai Y, Chen X, Liu W (2020) A review on raw materials, commercial production and properties of lyocell fiber. Journal of Bioresources and Bioproducts.

Kalia S, Dufresne A, Cherian BM, Kaith B, Avérous L, Nassiopoulos NJ (2011) Cellulose-based bio-and nanocomposites: a review. Int J Polym Sci 2011:1–35

Köhler S, Liebert T, Schöbitz M, Schaller J, Meister F, Günther W, Heinze T (2007) Interactions of ionic liquids with polysaccharides 1. Unexpected acetylation of cellulose with 1-ethyl-3-methylimidazolium acetate. Macromol Rapid Commun 28:2311–2317

Laidler KJ (1984) The development of the arrhenius equation. J Chem Educ 61:494–498

Lakes R, Drugan W (2002) Dramatically stiffer elastic composite materials due to a negative stiffness phase? J Mech Phys Solids 50:979–1009

Liang Y, Hawkins JE, Ries ME, Hine PJ (2021) Dissolution of cotton by 1-ethyl-3-methylimidazolium acetate studied with time–temperature superposition for three different fibre arrangements. Cellulose 28:715–727

Liebner F, Patel I, Ebner G, Becker E, Horix M, Potthast A, Rosenau T (2010) Thermal aging of 1-alkyl-3-methylimidazolium ionic liquids and its effect on dissolved cellulose. Holzforschung 64:25

Liu H, Cheng G, Kent M, Stavila V, Simmons BA, Sale KL, Singh S (2012) Simulations reveal conformational changes of methylhydroxyl groups during dissolution of cellulose Iβ in ionic liquid 1-ethyl-3-methylimidazolium acetate. J Phys Chem B 116:8131–8138

Luo Y (2021) Isotropized Voigt-Reuss model for prediction of elastic properties of particulate composites. Mechanics of Advanced Materials and Structures 1–13.

Meredith J, Coles SR, Powe R, Collings E, Cozien-Cazuc S, Weager B, Müssig J, Kirwan K (2013) On the static and dynamic properties of flax and Cordenka epoxy composites. Compos Sci Technol 80:31–38

Mwaikambo LY, Ansell MP (2001) The determination of porosity and cellulose content of plant fibers by density methods. J Mater Sci Lett 20:2095–2096

Nam S, French AD, Condon BD, Concha M (2016) Segal crystallinity index revisited by the simulation of X-ray diffraction patterns of cotton cellulose Iβ and cellulose II. Carbohyd Polym 135:1–9

Nevell TP, Zeronian SH (1985) Cellulose chemistry and its applications.

Ohira K, Abe Y, Kawatsura M, Suzuki K, Mizuno M, Amano Y, Itoh T (2012) Design of cellulose dissolving ionic liquids inspired by nature. Chemsuschem 5:388–391

Pinkert A, Marsh KN, Pang S, Staiger MP (2009) Ionic liquids and their interaction with cellulose. Chem Rev 109:6712–6728

Ries ME, Radhi A, Keating AS, Parker O, Budtova T (2014) Diffusion of 1-ethyl-3-methyl-imidazolium acetate in glucose, cellobiose, and cellulose solutions. Biomacromol 15:609–617

Rusznák I, Huszár A, Bodor G, Székely G, Trézl L, Serfőző G, Zaoui I (1975) Analysis of the orientation of polypropylene-based sheets suitable for fibrillated yarn production. Periodica Polytech, Chem Eng 19:201–217

Sayyed AJ, Deshmukh NA, Pinjari DV (2019) A critical review of manufacturing processes used in regenerated cellulosic fibres: viscose, cellulose acetate, cuprammonium, LiCl/DMAc, ionic liquids, and NMMO based lyocell. Cellulose 26:2913–2940

Sescousse R, Le KA, Ries ME, Budtova T (2010) Viscosity of cellulose−imidazolium-based ionic liquid solutions. J Phys Chem 114:7222–7228

Seydibeyoğlu MÖ, Oksman K (2008) Novel nanocomposites based on polyurethane and micro fibrillated cellulose. Compos Sci Technol 68:908–914

Shen L, Patel MK (2010) Life cycle assessment of man-made cellulose fibres. Lenzinger Berichte 88:1–59

Sun CC (2005) True density of microcrystalline cellulose. J Pharm Sci 94:2132–2134

Sun N, Rahman M, Qin Y, Maxim ML, Rodríguez H, Rogers RD (2009) Complete dissolution and partial delignification of wood in the ionic liquid 1-ethyl-3-methylimidazolium acetate. Green Chem 11:646–655

Swatloski RP, Spear SK, Holbrey JD, Rogers RD (2002) Dissolution of cellose with ionic liquids. J Am Chem Soc 124:4974–4975

Walden P (1914) Molecular weights and electrical conductivity of several fused salts. Bull. Acad. Imper. Sci.(St. Petersburg) 1800.

Woodings C (2001) A brief history of regenerated cellulosic fibers. Regenerated cellulose fibers 1–21.

Zavrel M, Bross D, Funke M, Büchs J, Spiess AC (2009) High-throughput screening for ionic liquids dissolving (ligno-) cellulose. Biores Technol 100:2580–2587

Zhang X, Ries ME, Hine PJ (2021) Time–Temperature Superposition of the Dissolution of Silk Fibers in the Ionic Liquid 1-Ethyl-3-methylimidazolium Acetate. Biomacromolecules.

Zhao Q, Yam RC, Zhang B, Yang Y, Cheng X, Li RKJC (2009) Novel all-cellulose ecocomposites prepared in ionic liquids. Cellulose 16:217–226

Zhu C, Richardson RM, Potter KD, Koutsomitopoulou AF, van Duijneveldt JS, Vincent SR, Wanasekara ND, Eichhorn SJ, Rahatekar SS (2016) High modulus regenerated cellulose fibers spun from a low molecular weight microcrystalline cellulose solution. ACS Sustain Chem Eng 4:4545–4553

Zugenmaier P (2001) Conformation and packing of various crystalline cellulose fibers. Prog Polym Sci 26:1341–1417

Zweckmair T, Hettegger H, Abushammala H, Bacher M, Potthast A, Laborie M-P, Rosenau T (2015) On the mechanism of the unwanted acetylation of polysaccharides by 1, 3-dialkylimidazolium acetate ionic liquids: part 1—Analysis, acetylating agent, influence of water, and mechanistic considerations. Cellulose 22:3583–3596